



## Article

# Evaluation of Spatiotemporal Patterns and Water Quality Conditions Using Multivariate Statistical Analysis in the Yangtze River, China

Jing Lu <sup>1,\*</sup>, Jiarong Gu <sup>1</sup>, Jinyang Han <sup>2</sup> , Jun Xu <sup>1</sup>, Yi Liu <sup>1</sup>, Gengmin Jiang <sup>1</sup> and Yifeng Zhang <sup>3</sup> 

<sup>1</sup> College of Civil Engineering and Architecture, Nanyang Normal University, Nanyang 473061, China; g15893021820@163.com (J.G.); xujunhit@126.com (J.X.); g230818@163.com (Y.L.); jianggengmin2013@126.com (G.J.)

<sup>2</sup> School of Chemistry and Chemical Engineering, Queen's University Belfast, David Keir Building, Stranmillis Road, Belfast BT95AG, UK; jhan09@qub.ac.uk

<sup>3</sup> Department of Environmental and Resource Engineering, Technical University of Denmark, DK-2800 Lyngby, Denmark; yifz@env.dtu.dk

\* Correspondence: lu\_jing13@163.com

**Abstract:** As a crucial surface water resource, the Yangtze River has raised concerns about its water quality due to its importance in economic and social development, environmental conservation, and agricultural development. The principal component analysis (PCA), hierarchical clustering analysis (HCA), and the water quality index (WQI) were utilized to assess the overall condition and detect spatiotemporal patterns and the key parameters of water quality in the Yangtze River. All usage data were determined monthly from samples taken in 2021 at the 33 Yangtze River water quality monitoring stations. The results demonstrated that 85% of the monitoring stations in the whole Yangtze River were maintained at a “good” condition, with average WQI values ranging from 71.16 to 81.25. The water quality was slightly poorer in the summer, with 56.6% of monitoring stations being in “medium” condition. Spatially, there was a downward trend in the water quality from upstream to downstream. Two significant principal component scores (PCs) were produced as a result of PCA and HCA, explaining 60.3% of the total variance in the upstream, 67.4% in the transition zone, and 50.4% in the downstream, respectively. In addition, the middle–upper reaches of water quality were found to correlated with  $\text{COD}_{\text{Mn}}$ , whereas the water quality in the downstream were mainly influenced by TUR, TP, T, and DO. The results primarily motivated our understanding of the Yangtze River’s water quality status and suggested the main targets for water quality improvement in different monitoring areas.

**Keywords:** water quality parameters; water quality index (WQI); hierarchical cluster analysis (HCA); principal component analysis (PCA); seasonal distribution



**Citation:** Lu, J.; Gu, J.; Han, J.; Xu, J.; Liu, Y.; Jiang, G.; Zhang, Y. Evaluation of Spatiotemporal Patterns and Water Quality Conditions Using Multivariate Statistical Analysis in the Yangtze River, China. *Water* **2023**, *15*, 3242. <https://doi.org/10.3390/w15183242>

Academic Editor: Bommanna Krishnappan

Received: 13 August 2023

Revised: 1 September 2023

Accepted: 6 September 2023

Published: 12 September 2023



**Copyright:** © 2023 by the authors. Licensee MDPI, Basel, Switzerland. This article is an open access article distributed under the terms and conditions of the Creative Commons Attribution (CC BY) license (<https://creativecommons.org/licenses/by/4.0/>).

## 1. Introduction

Clean water is considered one of the most essential natural resources for ensuring the security of both human health and biodiversity [1,2]. However, as our society and economy advance, point source pollution, non-point source pollution, and air pollution all worsen water quality [3–5]. Surface water is severely polluted on a global scale [6–8]. Suspended solids, organic wastes, and nutrients make up major pollutants [9–11]. Different types of water contamination can be detected by water quality indices. For instance, high total phosphorus levels, a defining organic waste, may lead to eutrophication of water bodies and even bloom occurrence [12]. Therefore, a comprehensive understanding of the spatial–temporal variations of water quality parameters was necessary, as well as an objective assessment of water quality [13,14]. For the purpose of developing environmental protection and resource management policies, it is crucial to accurately gauge changes in

water quality and identify indicators of priority in various locations. In this regard, it is vital to filter out water quality assessment methods that can be generally used, are simple to compute, and produce reliable results.

Various water quality evaluation methods have been established for assessing water quality conditions, including the Analytic Hierarchy Process method [15]; the Nemerow index method [16]; the BP network model [17,18]; and the single factor index method [19]. Nevertheless, the monitoring of water quality usually generates a series of datasets, which must be converted into a format that can be simply and successfully interpreted [20]. Compared to other methods, principal component analysis (PCA) has been extensively applied for the assessment of water quality. PCA transforms a set of potentially correlated variables into a set of linearly uncorrelated variables, thereby removing correlation between evaluation indicators and reducing the workload associated with index selection [21]. When evaluation approaches are effectively combined, the assessment can more correctly reflect the water quality than when only one method is used [22]. Given that hierarchical cluster analysis (HCA) is an available tool to classify similar samples into various groups [23], the PCA method combining HCA is used to evaluate the Yangtze River's water quality, delineating the extent of water pollution in space.

The Yangtze River is the third-largest river in the world and the longest river in China [24]. The most significant economic hub and reservoir of natural resources in China is the Yangtze River Economic Belt, which was built around the Yangtze River [25]. More than half of the nation's wastewater is released into the Yangtze River each year, constituting a pollution belt along the shoreline that stretches approximately 600 km [26]. The Yangtze River basin's water contamination has increased due to wastewater discharge, which is hindering the basin's sustainable development [24]. A series of improvement measures has been taken to enhance the Yangtze River's water quality. The Chinese Academy of Environmental Sciences established the national Yangtze River Ecological Environment Protection and Restoration Joint Research Center in April 2018 [26]. Since 2019, the Chinese government has enforced laws for the prevention and management of water pollution in the Yangtze River basin. Additionally, the Yangtze River Protection Law was passed in December 2020 [27]. To quickly determine whether water quality prevention and control strategies are effective, a reliable water quality assessment is very important for the Yangtze River. Numerous studies have been carried out recently to investigate the Yangtze River's water quality situation [28–31]. Nevertheless, a lot of research solely pays attention to the Yangtze River's partial regions [29,30,32]. Focusing on the spatial and temporal distribution of water quality in the Yangtze River's main channel is essential, particularly after the implementation of various measures in 2020. We can comprehend the overall water quality of the Yangtze River and pinpoint the critical areas utilizing the principal component analysis and cluster analysis.

In this study, nine water quality parameters were chosen for our research from the 33 Yangtze River water quality monitoring stations in 2021. The specific objectives are as follows: (1) assess the overall water quality condition and understand spatiotemporal water quality patterns based on individual parameters; (2) identify the key water quality parameters of different segments by combining hierarchical cluster analysis and principal component analysis.

## 2. Materials and Methods

### 2.1. Study Region

The Yangtze River (90°33'~122°25' E, 24°30'~35°45' N) originates from the southwest side of Galadandong Peak of the Tanggula Mountains on the Qinghai–Tibet Plateau, with a total length of 6397 km. The main stream travels through 11 administrative regions of the provinces, including Shanghai, Jiangsu, Zhejiang, Anhui, Jiangxi, Hubei, Hunan, Chongqing, Sichuan, Yunnan, and Guizhou, before emptying into the East China Sea to the east of Chongming Island (Figure 1) (Table 1). Its main tributaries are the Yalong River, Minjiang River, Tuojiang River, Jialing River, etc. The main lakes are Dongting Lake, Poyang

Lake, Taihu Lake, etc. The Yangtze River basin’s yearly average precipitation ranges widely from west to east (300–2400 mm), and its annual average temperature also ranges widely (9–18 °C) [33]. The Qinghai–Tibet Plateau, which is characterized by an alpine climate, is where the basin’s source is located. This region experiences 300 mm of precipitation on average every year, with an average temperature of −4 °C [34]. The subtropical monsoon climate that prevails in the middle and lower reaches is characterized by hot, wet summers and warm, humid winters [35,36]. Forest reserves make up 25% of all the country’s woods in this region, and the area is rich in vegetative resources. The middle and downstream plains have a substantial amount of farmland [37].

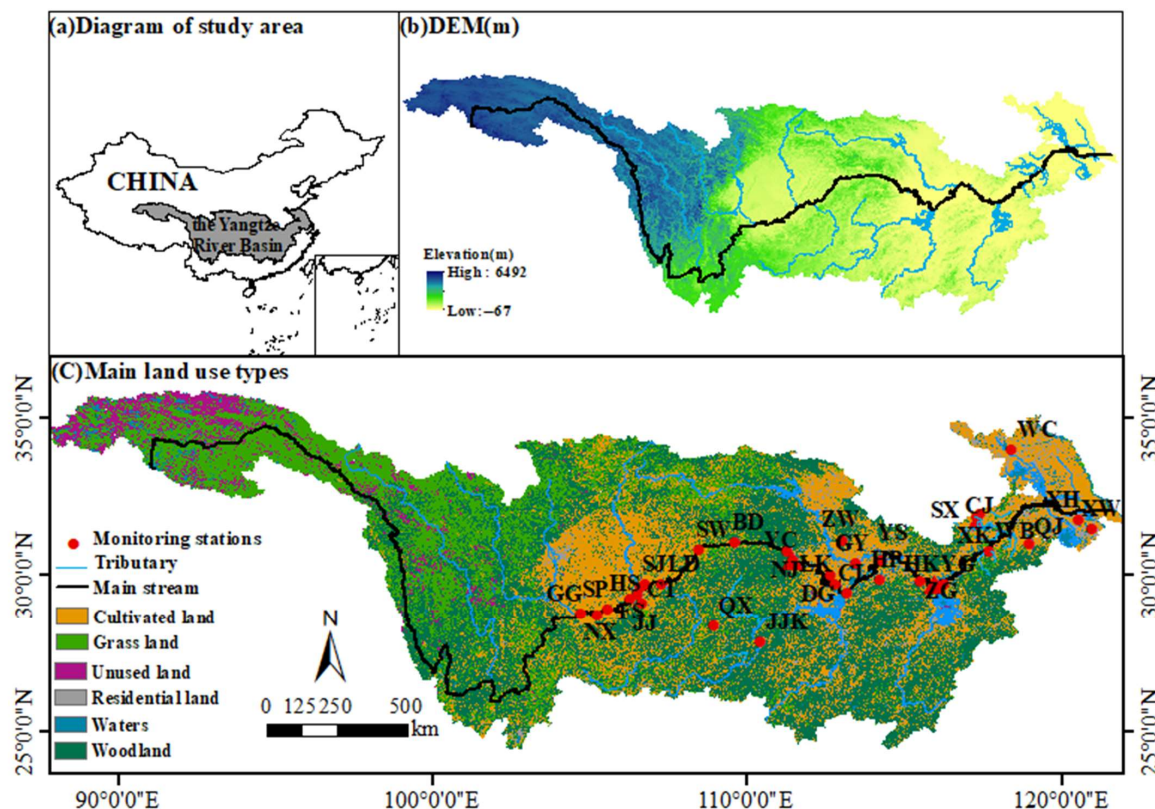


Figure 1. Location of the study area. (a) The location of the Yangtze River basin in China; (b) elevations; and (c) main land use types.

Table 1. Information on the water quality monitoring stations.

River Subdivision	Station	Abbreviation	Latitude (°)	Longitude (°)	Elevation (m)
The upstream stations	Guagongshan	GG	28.78	104.68	327
	Naxidadukou	NX	28.74	105.23	272
	Shoupayan	SP	28.90	105.55	221
	Jiangjindaqiao	JJ	29.26	106.26	181
	Fengshouba	FS	29.41	106.51	167
	Heshangshan	HS	29.12	106.64	437
	Cuntan	CT	29.62	106.60	163
	Sujia	SJ	29.75	106.72	368
	Lidu	LD	29.75	107.27	314
	Shaiwangba	SW	30.83	108.45	149
	Qingxichang	QX	28.41	108.92	395
	Jingjiangkou	JJK	27.87	110.39	145
	Baidicheng	BD	31.04	109.57	115
	Nanjinguan	NJ	30.76	111.27	57

Table 1. Cont.

River Subdivision	Station	Abbreviation	Latitude (°)	Longitude (°)	Elevation (m)
The middle stream stations	Yunchi	YC	30.48	111.46	67
	Diaoguan	DG	29.69	112.64	29
	Liukou	LK	29.74	112.76	36
	Chenglingji	CL	29.45	113.15	18
	Zhuanwachang	ZW	31.09	113.03	108
	Guanyinsi	GY	30.39	113.43	29
	Yangsigang	YS	30.51	114.26	26
	Huanglashi	HP	29.86	114.20	30
	Zhongguanpu	ZG	29.84	115.48	25
	Hukou	HK	29.74	116.26	31
The downstream stations	Yaoguang	YG	29.73	115.98	30
	Sanxingcun	SX	31.97	117.42	40
	Xiangkou	XK	31.86	117.28	18
	Chenjiadun	CJ	31.59	117.27	7
	Wubugou	WB	30.77	117.68	12
	Weicun	WC	34.00	118.42	20
	Qianjiangkou	QJ	31.02	118.95	19
	Xiaohekou	XH	31.78	120.55	2
	Xiaowan	XW	31.49	120.99	3

## 2.2. Datasets

In this study, the Yangtze River's 33 water quality monitoring stations, which cover the main stream and important tributaries, collected water samples on a monthly basis in 2021 (Figure 1). Meanwhile, 14 water quality monitoring stations (from Guagongshan to Nanjinguan station) are located upstream of the Yangtze River, 10 water quality monitoring stations (from Yunchi to Hukou station) are located in the middle stream of the Yangtze River, and 9 water quality monitoring stations (from Yaoguan to Xiaowan station) are located downstream of the Yangtze River. Nine water quality parameters were analyzed in our study, including pH (unitless), dissolved oxygen (DO, mg/L), potassium permanganate index ( $\text{COD}_{\text{Mn}}$ , mg/L), ammonia nitrogen ( $\text{NH}_3\text{-N}$ , mg/L), temperature ( $T$ , °C), electrical conductivity (EC,  $\mu\text{S}/\text{cm}$ ), turbidity (TUR, NTU), total phosphorus (TP, mg/L), and total nitrogen (TN, mg/L), respectively. A total of 3564 samples were collected. The water samples were obtained from the Ministry of Ecology and Environment of the People's Republic of China (<https://www.mee.gov.cn/>) (accessed on 10 September 2022). Sampling methods refer to the standard for water quality sampling—technical regulation of the preservation and handling of samples [38]. The methods for sample chemistry analyses were based on the *Standard Methods for the Examination of Water and Wastewater* [39]. Additionally, duplicate and blank samples were collected at each station to check the analytical accuracy. To analyze seasonal changes in water quality, the seasons were defined as spring, summer, autumn, and winter, corresponding to the periods of March to May, June to August, September to November, and December to February, respectively. Meanwhile, the study area's border data are provided by the Resource and Environment Science and Data Center, China (<https://www.resdc.cn/>) (accessed on 1 October 2022).

## 2.3. Methods

### 2.3.1. Water Quality Index (WQI)

The WQI proposed by Rodriguez de Bassoon [40] has been widely used for water quality assessment [41–43]. Water parameters were assigned weighting factors, which could represent the difference of importance [40]. The calculations are based on the following equation:

$$\text{WQI} = \frac{\sum_{i=1}^n C_i P_i}{\sum_{i=1}^n P_i}$$



where  $n$  is the total number of water quality parameters,  $C_i$  is the normalized value of the  $i$ -th parameter based on Rodriguez de Bassoon (Table 2) [40], and  $P_i$  is the  $i$ -th parameter’s calculated weight that is displayed in Table 2 after being validated by earlier studies. [40,44]. According to  $WQI$  values, water quality was divided into five categories: excellent (91–100), good (71–90), medium (51–70), bad (26–50), and very bad (0–25).

**Table 2.** The relative weights and the normalization factors of the parameters.

Variables <sup>a</sup>	Weight (Pi)	Normalization Factor (Ci)										
		100	90	80	70	60	50	40	30	20	10	0
pH	1	7	[7, 8)	[8, 8.5)	[8.5, 9)	[6.5, 7)	6–6.5, 9, 9.5	5, 6, 9.5, 10	4–5, 10–11	3–4, 11–12	2–3, 12–13	1–2, 13–14
DO	4	>7.5	[7, 7.5)	[6.5, 7)	[6, 6.5)	[5, 6)	[4, 5)	[3.5, 4)	[3, 3.5)	[2, 3)	[1, 2)	<1
COD <sub>Mn</sub>	3	<1	[1, 2)	[2, 3)	[3, 4)	[4, 6)	[6, 8)	[8, 10)	[10, 12)	[12, 14)	[14, 15)	>15
NH <sub>3</sub> -N	3	<0.01	[0.01, 0.05)	[0.05, 0.10)	[0.10, 0.20)	[0.20, 0.30)	[0.30, 0.40)	[0.40, 0.50)	[0.50, 0.75)	[0.75, 1.00)	[1.00, 1.25)	>1.25
T	1	16–21	15–16, 21–22	14–15, 22–24	12–14, 24–26	10–12, 26–28	5–10, 28–30	0–5, 30–32	–2–0, 32–36	–4–2, 36–40	–6–4, 40–45	>45, <–6
EC	1	<750	[750, 1000)	[1000, 1250)	[1250, 1500)	[1500, 2000)	[2000, 2500)	[2500, 3000)	[3000, 5000)	[5000, 8000)	[8000, 12,000)	>12,000
TUR	2	<5	[5, 10)	[10, 15)	[10, 20)	[20, 25)	[25, 30)	[30, 40)	[40, 60)	[60, 80)	[80, 100)	>100
TP	1	<0.01	[0.01, 0.02)	[0.02, 0.05)	[0.05, 0.1)	[0.1, 0.15)	[0.15, 0.2)	[0.2, 0.25)	[0.25, 0.3)	[0.3, 0.35)	[0.35, 0.4)	>0.4
TN	2	<0.1	[0.1, 0.2)	[0.2, 0.35)	[0.35, 0.5)	[0.5, 0.75)	[0.75, 1)	[1, 1.25)	[1.25, 1.5)	[1.5, 1.75)	[1.75, 2)	>2

Note: <sup>a</sup> Values in mg/L, T as °C, EC as S/cm, and TUR as NTU.

### 2.3.2. Hierarchical Cluster Analysis (HCA)

Cluster analysis, which is used to reveal the correlation or similarity between objects [45], could group the objects into few classes. The same classes have similar characteristics but are different from other classes. Hierarchical cluster analysis was chosen in our study. Cluster analysis has been widely used in water quality research [46,47]. The main steps of hierarchical cluster analysis are as follows:

1. Data standardization using Z-source method

$$Z_{ij} = \frac{X_{ij} - X_i}{S_i}$$

where  $Z_{ij}$  is the water quality index’s variable value following normalization at each monitoring station,  $X_{ij}$  is the average annual observed water quality concentration index value of each monitoring station,  $X_i$  is the mathematical expectation, and  $S_i$  is standard deviation;

2. Treat  $n$  samples as their own category;
3. Combine the two classes with the smallest distance to form the new class. Distance calculation usually uses Euclidean distance;
4. Calculate the clustering distance between the new class and other types;
5. Continue to combine the two most recent categories;
6. Repeat until all samples are in the same category.

### 2.3.3. Principal Component Analysis (PCA)

Principal component analysis was first introduced by Karl Pearson for non-random variables and depends on an eigenvector decomposition of the covariance or correlation matrix to establish combinations of variables [48]. In brief, PCA transforms a raw dataset to a new orthogonal uncorrelated variables dataset [49]. PCA is a common dimensionality reduction method, whereby a close distance between two samples indicates a similar species composition. The correlation matrix is adopted for the PCA, which signifies that all

9 parameters are assigned equal weights in forming the principal components. The main steps of PCA are as follows:

1. Standardize the raw data;
2. Calculate the correlation coefficient matrix  $C$ ;

$$C = \frac{1}{n-1} X_t X_t^T, n = 9$$

3. Calculate the eigenvalues and eigenvectors;
4. Calculate principal component contribution rate and cumulative contribution rate;
5. Select the first  $K$  principal components according to the cumulative contribution rate of each component points:

$$P = \begin{bmatrix} P_1^T \\ P_2^T \\ \vdots \\ P_n^T \end{bmatrix}$$

where  $n$  represents the number of dimensions,  $X_t$  represents the matrix after preprocessing,  $P$  represents the cumulative contribution rate, and  $P_1$  through  $P_n$  represent the  $N$ th principal component.

In our study, the data of PCA should be preprocessed using a hierarchical cluster analysis. All mathematical and statistical computations were made using IBM SPSS Statistics 27 and Origin (Origin Pro 2023 (64-bit) 10.0.0.154).

### 3. Results

#### 3.1. Water Quality Assessment of the Yangtze River

As a non-parametric statistical method, this paper cites Kruskal–Wallis as a difference significance test [50]. Table 3 displays the statistical calculation summary of the quarterly mean of the river. Figures 2 and 3 present variations in the spatial–temporal concentrations of nine water quality parameters of the Yangtze River, respectively.

**Table 3.** Comparison of the variations of the water quality parameters in the Yangtze River in 2021.

Parameters <sup>a</sup>		pH	DO	COD <sub>Mn</sub>	NH <sub>3</sub> -N	T	EC	TUR	TP	TN
Thresholds of the Class I Standards <sup>b</sup>		6.00~9.00	≥7.50 mg/L	≤2.00 mg/L	≤0.15 mg/L	N/A	N/A	N/A	≤0.02 mg/L	≤0.20 mg/L
Spring	Avg. ± S.D.	7.82 ± 0.26	8.54 ± 1.01	1.43 ± 0.39	0.058 ± 0.039	17.30 ± 2.76	373.35 ± 59.73	27.19 ± 20.17	0.064 ± 0.019	1.893 ± 0.339
	Max	8.31	9.71	2.33	0.15	19.50	469.43	69.90	0.13	2.75
	Min	7.25	6.19	0.76	0.02	14.12	249.56	3.75	0.03	1.14
	H	29.14	234.14	111.17	27.89	354.02	52.22	169.41	51.58	48.31
	P	0.004	<0.001	<0.001	<0.001	<0.001	<0.001	<0.001	<0.001	<0.001
Summer	Avg. ± S.D.	7.72 ± 0.29	7.00 ± 1.23	1.99 ± 0.74	0.055 ± 0.078	25.32 ± 2.46	342.17 ± 47.16	86.91 ± 73.68	0.075 ± 0.027	1.799 ± 0.432
	Max	8.27	8.95	3.50	0.37	28.14	420.66	262.57	0.13	2.43
	Min	7.16	2.89	1.07	0.02	18.19	267.70	9.40	0.04	0.91
	H	31.94	239.84	117.34	24.6	354.103	54.89	189.06	56.27	44.92
	P	0.001	<0.001	<0.001	<0.001	<0.001	<0.001	<0.001	<0.001	<0.001
Autumn	Avg. ± S.D.	7.78 ± 0.25	7.95 ± 1.14	1.93 ± 0.62	0.055 ± 0.065	21.50 ± 3.71	347.03 ± 37.98	55.07 ± 42.57	0.065 ± 0.022	1.656 ± 0.389
	Max	8.19	9.56	3.31	0.31	23.61	421.19	160.58	0.12	2.49
	Min	7.29	4.91	0.97	0.02	14.62	288.05	13.94	0.02	1.00
	H	29.62	229.63	117.38	24.38	351.64	54.22	179.44	51.65	48.31
	P	0.003	<0.001	<0.001	<0.001	<0.001	<0.001	<0.001	<0.001	<0.001
Winter	Avg. ± S.D.	7.89 ± 0.25	9.62 ± 1.13	1.48 ± 0.60	0.057 ± 0.049	13.74 ± 2.75	381.72 ± 47.70	23.71 ± 20.90	0.061 ± 0.023	1.727 ± 0.337
	Max	8.26	11.14	3.13	0.23	20.19	462.23	70.27	0.13	2.25
	Min	7.46	7.62	0.85	0.02	10.56	296.15	3.31	0.023	1.00
	H	33.35	247.03	109.30	26.27	352.24	58.34	171.43	52.30	45.77
	P	0.001	<0.001	<0.001	<0.001	<0.001	<0.001	<0.001	<0.001	<0.001

Notes: <sup>a</sup> Values in mg/L, T as °C, EC as S/cm, and TUR as NTU. <sup>b</sup> Standards from the People’s Republic of China’s environmental quality regulations for surface water [51]).

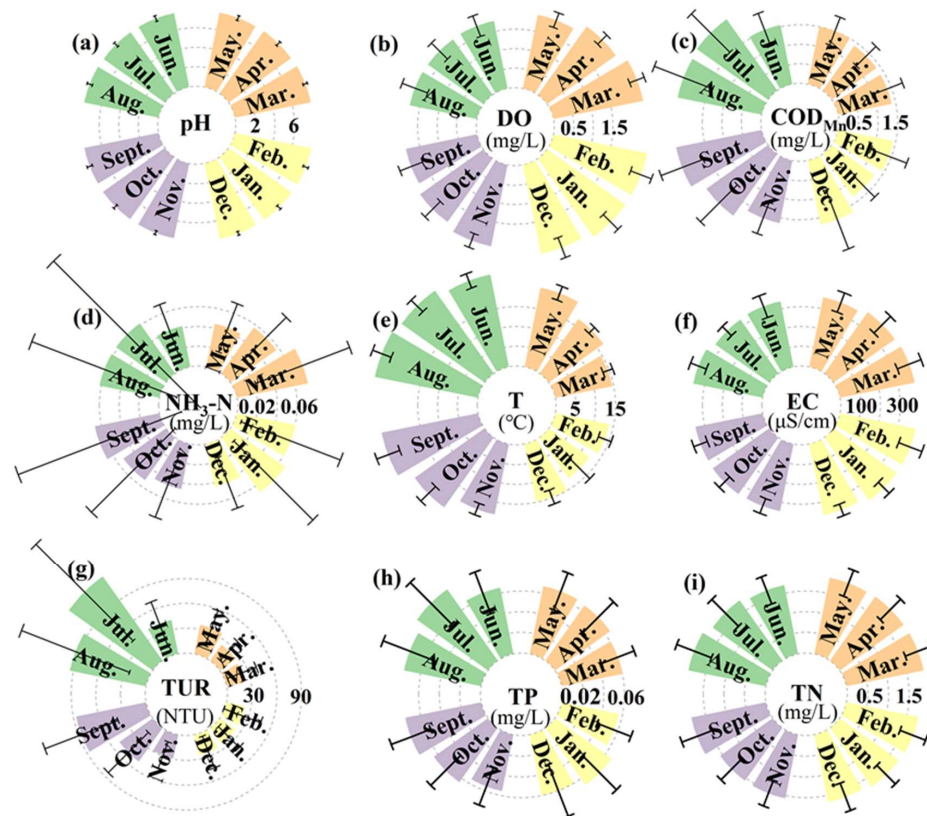


**Figure 2.** Temporal concentrations for 9 water quality parameters for each monitoring station of the Yangtze River. Note: (1) (a–i) represent the monthly water quality data for pH, DO,  $\text{COD}_{\text{Mn}}$ ,  $\text{NH}_3\text{-N}$ , T, EC, TUR, TP, and TN, respectively; (2) range represents spring; green represents summer; purple represents autumn; and yellow represents winter.

### 3.1.1. Water Quality Temporal Conditions Based on Physicochemical Properties

The quarterly mean pH values were all greater than 7.72, while the maximum measured pH value occurred in the spring (Table 3). All of the average pH readings over the course of a year were higher than 6.94 (Figure 2a). The lowest and highest values for dissolved oxygen were 6.96 mg/L in July and 9.81 mg/L in January, respectively ( $p < 0.005$ , Table 3) (Figure 2b). Algal blooms and warmth are likely to blame for the shift in dissolved oxygen content [52]. From September to April, there was a clear reduction in the monthly  $\text{COD}_{\text{Mn}}$  values (Figure 2c). The  $\text{NH}_3\text{-N}$  values in the successive months (January to March and July to September) were relatively higher than those in the previous months (Figure 2d), and 13.74 °C and 25.32 °C were the greatest and lowest quarterly mean T values, respectively (Table 3). According to Figure 2e, the temporal variation exhibited a clear increased tendency from March to September and a downward trend from October to February, which is consistent with China's overall temperature trend. It might have something to do with atmospheric precipitation [53]. The highest and minimum EC values varied by at least 1.5 times over each season. But there was no discernible change in EC from spring to winter (Figure 2f). The greatest quarterly mean for TUR, which is reliant on seasonal changes, was 86.91 NTU in the summer. For NTU, there was a significant difference in value across the months ( $p < 0.005$ , Table 3) (Figure 2g). Heavy rainfall, run-off with a high suspended matter content, and organic matter pollution could all have an impact. TP concentrations were greatly above the Class I standard of the People's Republic of China's environmental quality regulations for surface water (GB 3838-2002) of 0.02 mg/L (Figure 2h). There was no discernible temporal change in TN, with the highest TN value of 1.92 mg/L occurring in August (Figure 2i).

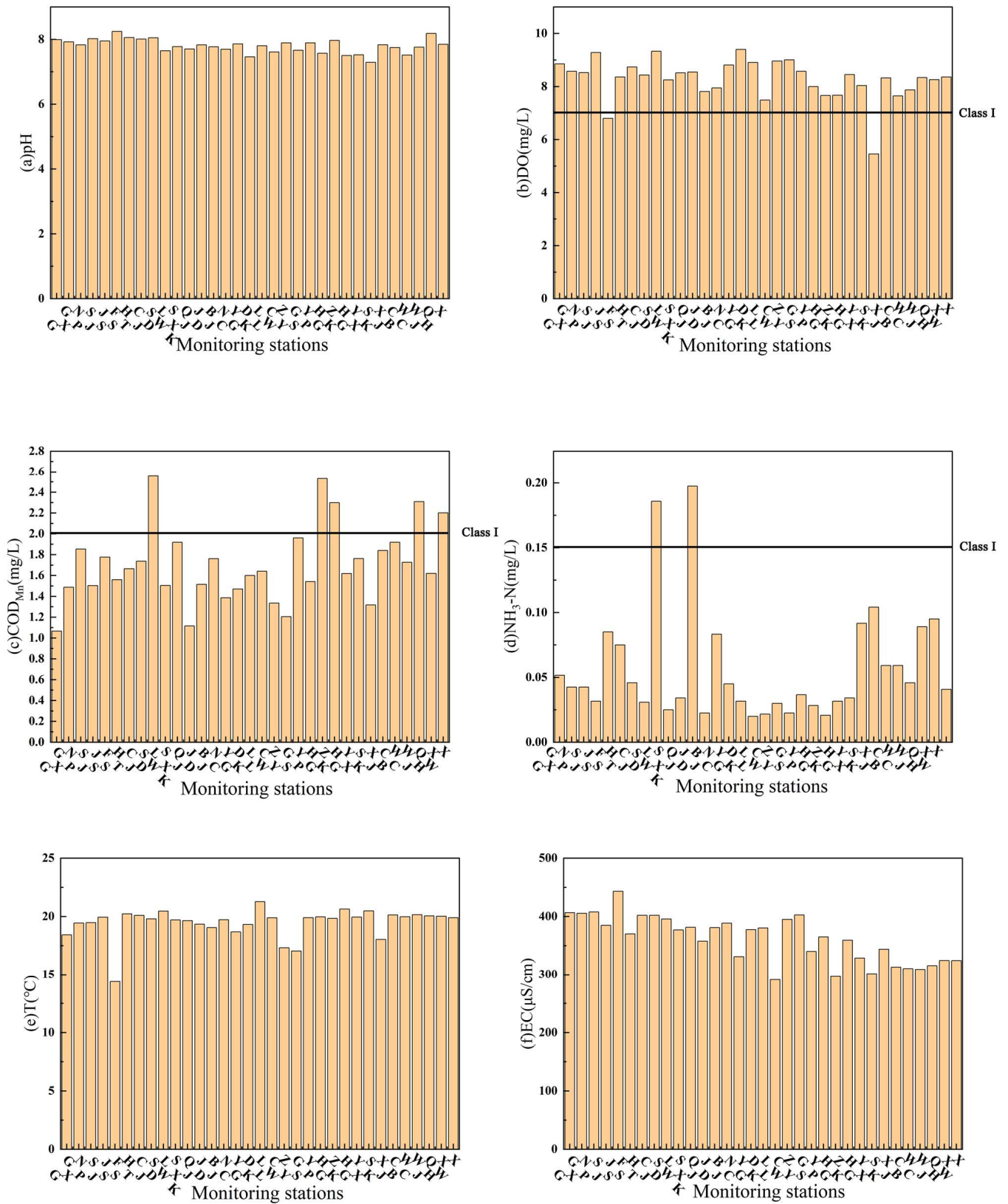
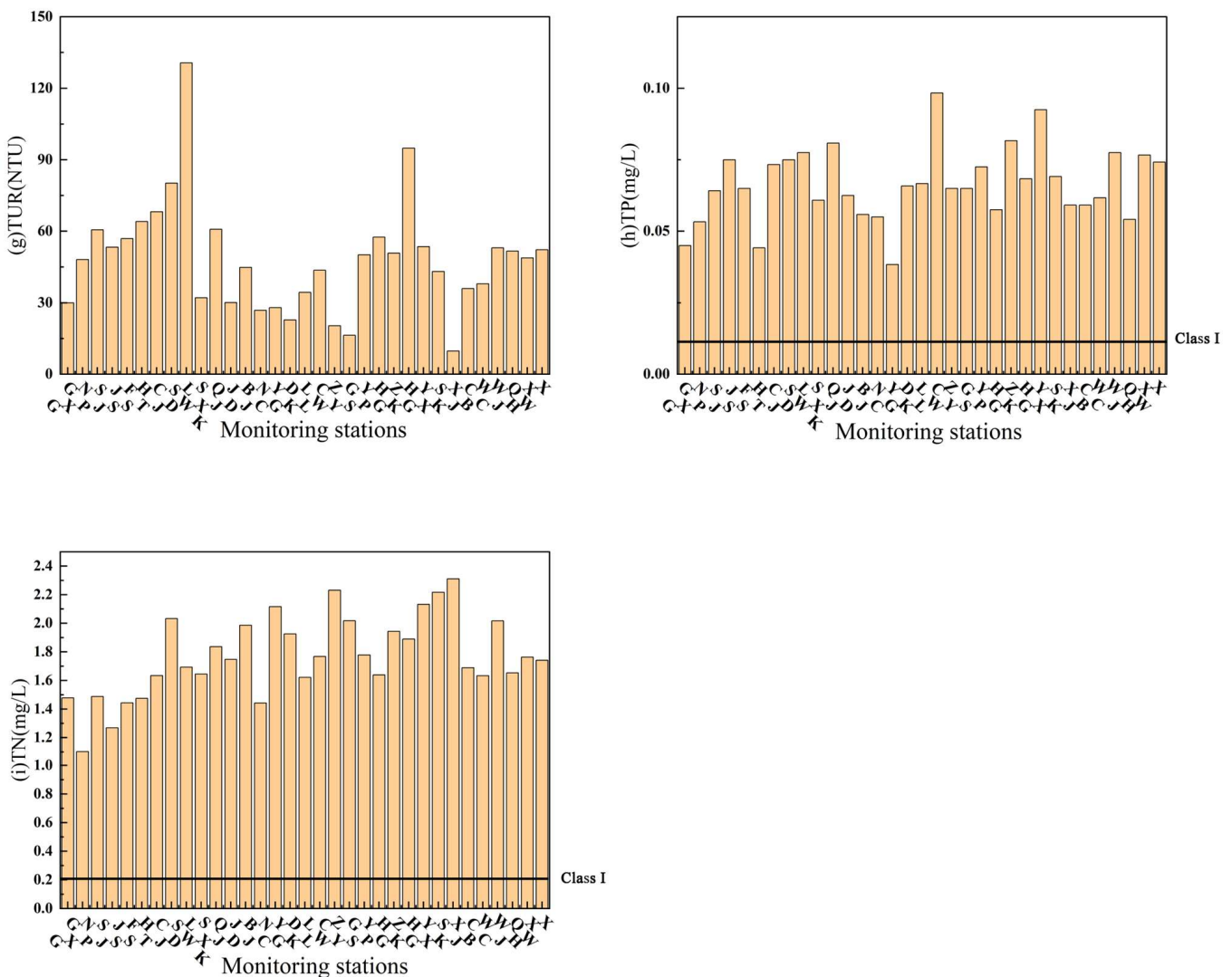


Figure 3. Cont.





**Figure 3.** Average concentrations for 9 water quality parameters for each water quality monitoring station in the Yangtze River in 2021.

### 3.1.2. Water Quality Patterns Based on Spatial Variation

The Yangtze River basin’s regional distribution of water quality data is shown in Figure 3. The distribution of the pH values showed a hidden trend with fluctuations from upstream to downstream, and the average pH values were larger than 7.3 at 33 successive stations (from the GG station to the XW station) (Figure 3a). The DG station recorded the highest DO values at 9.4 mg/L, whereas the XK station recorded the lowest at 5.46 mg/L (Figure 3b). The average yearly concentration of COD<sub>Mn</sub> downstream was 1.81 mg/L. Nearly ten times as much NH<sub>3</sub>-N was present at the LK station’s maximum value than at the JJK station’s lowest (Figure 3d). There was no discernible pattern for T across all stations. T values ranged from 7.69 °C in the winter at the XK station to 29.65 °C in the summer at the SX station (Figure 3e). EC showed an obvious decreasing trend from upstream to downstream, ranging from 406.6 ± 31.8 μS/cm at the GG station to 324.3 ± 38.2 μS/cm at the XW station (Figure 3f). The TUR contents in the upstream stations were higher than those of the other stations, with the LD station having the highest value at 130.7 111.2 NTU and the XK station having the lowest value at 9.7 3.1 NTU (Figure 3g). The TP values from upstream to downstream did not appear to vary spatially. At the CL station, the highest TP values were 0.10 mg/L (Figure 3h). The distribution of the TN concentrations following 33 consecutive stations presented over 0.2 mg/L.

### 3.1.3. Water Quality Conditions Based on WQI

Figure 4 depicts variations in water quality conditions. The WQI was calculated in the Yangtze River during sampling periods based on the nine measured water quality parameters above. From spring through winter, the Yangtze River's WQI value first declined and then rose. In the spring, summer, autumn, and winter, the mean WQI values were 75, 61, 67, and 73, respectively. The maximum WQI value was 79.70 in November, and the minimum WQI value was 67.44 in July. The results demonstrate that the water quality was slightly poor in the summer, with 56.60% of monitoring stations rated as "average". Spatially, the water quality presented a trend of deterioration from upstream to downstream. The stations downstream had a score ranging from 68.80 to 74.03. The majority (85%) of monitoring stations' WQI scores, with WQI values ranging from 71.16 to 81.25, classed the water quality conditions as "good". The minimum WQI value was 68.80 at the XK station, and it was classified as "average" along with the LD station and the HK station. Overall, the Yangtze River's water quality is "good" based on the WQI results.

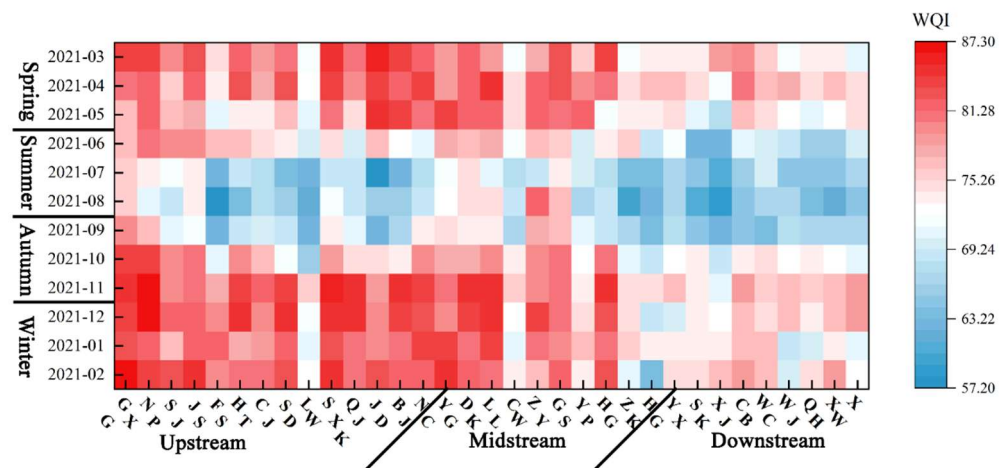


**Figure 4.** Spatial and temporal variations in the WQI of the Yangtze River in 2021.

## 3.2. Analysis of Water Quality Patterns of the Yangtze River Using the PCA Method

### 3.2.1. Hierarchical Cluster Analysis (HCA) of Yangtze River Water Quality

According to the similarity of the dataset and the identification of similarities and differences, hierarchical cluster analysis (HCA) is a tool that can be used to arrange similar samples into various groups [54,55]. In our study, the HCA was conducted on standardized data to examine spatial differences and correspondence between 33 stations along the river. The circular dendrogram (Figure 5) shows the three primary patterns that were found. About 45% of the data came from the monitoring stations of the first groups, which were primarily located upstream of the Yangtze River. The second group, with only one-third as many monitoring stations as the first group, was mostly situated in the upstream–downstream transition zone. The third group was mainly composed of the downstream stations including about 39% of all stations.

### 3.2.2. Water Quality Conditions Patterns Based on the PCA

The PCA, which could identify some noteworthy parameters, was used to explore the contribution of different parameters to water quality status in different patterns identified using the hierarchical cluster analysis. The outcomes are displayed in Table 4 and Figure 6. The PCA using annual data revealed that the first two PCs explained more than 52.76% of the total variance of the water quality (Figure 6d). PC1 had a significant negative association with EC and a relatively greater positive correlation with  $COD_{Mn}$ , indicating that PC1 is associated with cleanliness of the sediment and organic pollution. Comparatively speaking, the Yangtze River's water quality can be controlled by paying more attention to the impact

of organic contaminants and water acidity, according to the strong correlation between PC2, pH, and TN.

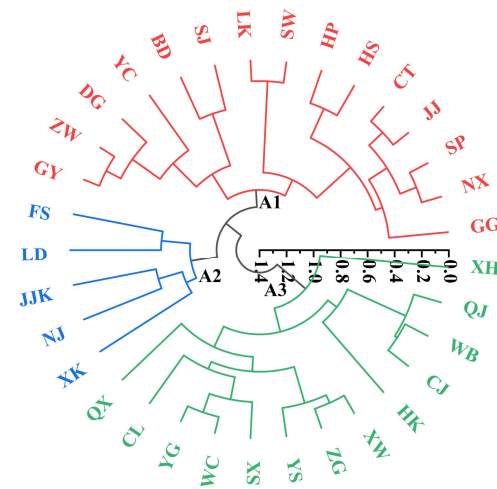


**Figure 5.** Dendrogram showing results of hierarchical cluster analysis of quality of monitoring stations in the Yangtze River.

**Table 4.** Factor loadings of principal components on variables.

Variables	A <sup>a</sup>		A1 <sup>a</sup>		A2 <sup>a</sup>		A3 <sup>a</sup>	
	PC1	PC2	PC1	PC2	PC1	PC2	PC1	PC2
pH	−0.241	0.557	−0.177	0.609	0.435	−0.337	0.272	−0.054
DO	−0.366	0.224	−0.403	−0.084	0.291	−0.278	0.483	0.360
COD <sub>Mn</sub>	0.422	0.312	0.459	0.111	0.446	0.126	−0.286	0.250
NH <sub>3</sub> -N	0.010	0.117	−0.152	0.479	0.169	0.270	0.288	−0.317
T	0.460	0.008	0.470	0.086	0.144	0.482	−0.512	−0.250
EC	−0.373	0.291	−0.277	0.137	0.166	−0.462	0.366	0.289
TUR	0.401	0.436	0.441	0.237	0.480	0.251	−0.319	0.419
TP	0.331	0.167	0.283	−0.076	0.370	0.303	−0.173	0.568
TN	0.088	−0.475	−0.019	−0.541	−0.287	0.346	0.003	0.247
Eigenvalue (%)	34.239	18.525	42.995	17.256	35.719	31.725	31.987	18.437
Cumulative (%)	34.239	52.764	42.995	60.251	35.719	67.444	31.987	50.424

Note: <sup>a</sup> A denotes the entire Yangtze River, A1 the upstream zone, A2 the upstream–downstream transition zone, and A3 the downstream zone.

More than 60% of the overall variance in the water quality was explained by the first two principal components (PCs) in the first group. A total of 43.0% of the variation was supplied by the first and greatest eigenvector, and 17.3% was supplied by the second. PC1 had comparatively higher positive correlations with T, followed by COD<sub>Mn</sub> and TUR. PC2 had a high correlation with pH and TN. The winter was distinct from the summer (Figure 6a). Specifically, summer had distinctive water quality with relatively high correlations between DO and EC, and winter had relatively high positive correlations between COD<sub>Mn</sub>, TUR, and T (Figure 6a).

In the second group, PCA produced a two-component model explaining 67.44% of the variation in the water quality overall. The first main component (PC1), which had larger loadings with TUR, COD<sub>Mn</sub>, and pH, accounted for 35.7% of the variability in total. PC2, which has a correlation with EC and T, is responsible for 31.7% of the overall variation. The temporal difference of A2 was inconspicuous, relatively speaking (Figure 6b). A significant level of consistency was seen when the PCA results of the transition zone were compared to those of the upstream region. Higher correlations between TUR, COD<sub>Mn</sub>, and T and water

quality show the impact of organic matter and sediment in the upstream and transitional regions.

The first two PCs in the third group accounted for 50.42% of the overall variance in the water quality. The coefficients of parameters demonstrated that T had a relatively high negative correlation, and DO had a higher positive correlation with PC1. TP and TUR had positive correlations with PC2 (Figure 6c). Therefore, the downstream water quality was mainly affected by phosphorus-containing pollutants, suspended sediments, or algae. Compared with other seasons, the similarities between spring and fall are considerable.

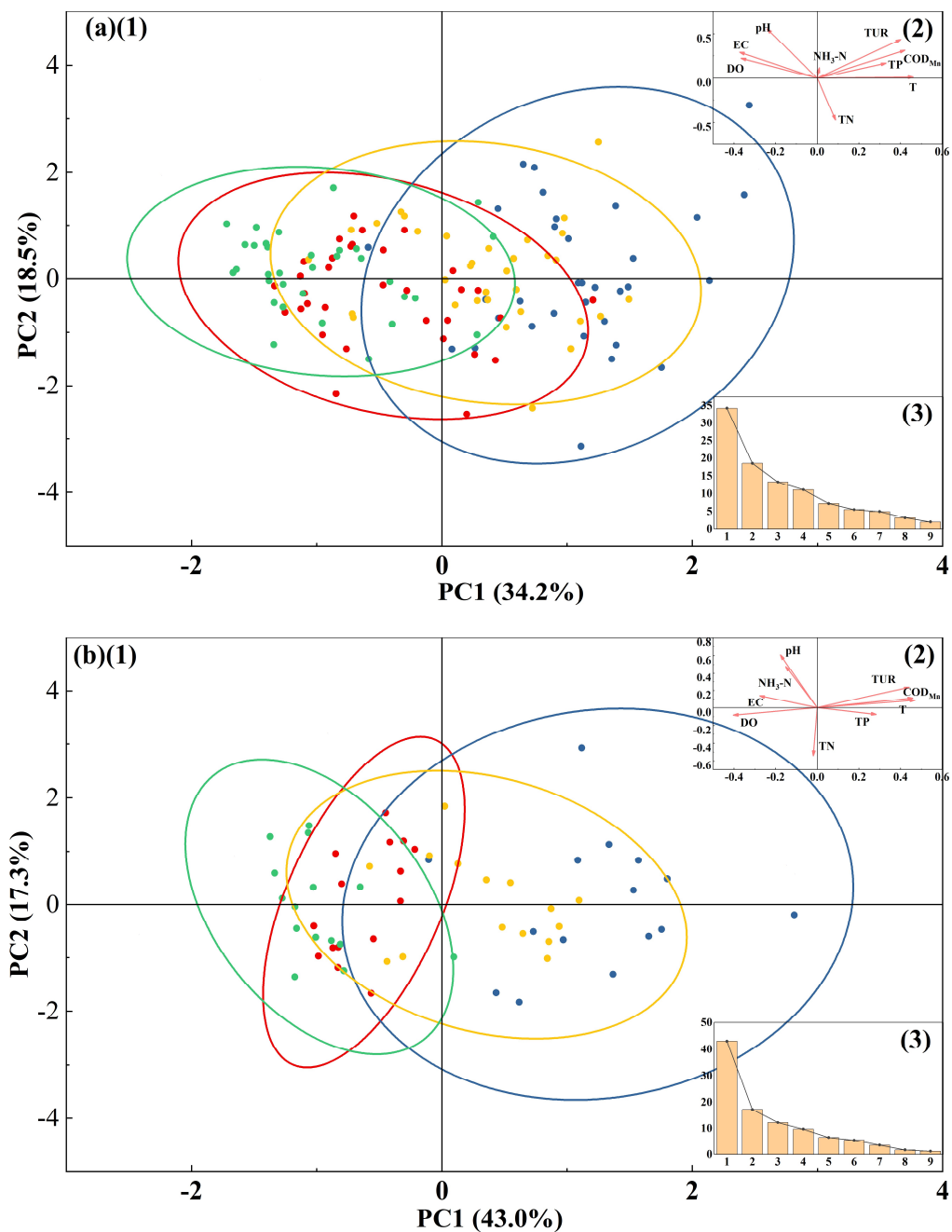
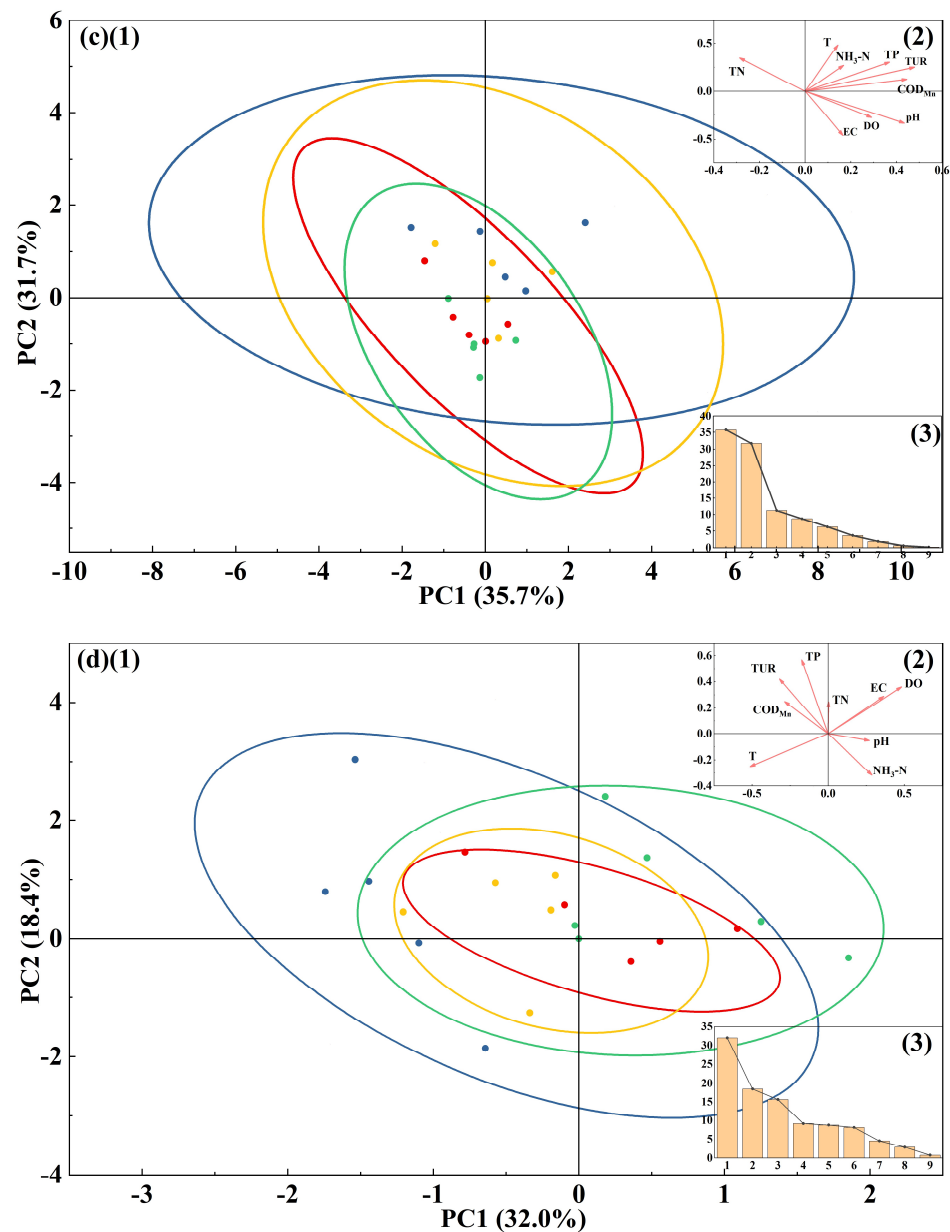


Figure 6. Cont.





**Figure 6.** Water quality patterns in (a) A, (b) A1, (c) A2, and (d) A3 in the Yangtze River. Note: (1) The PCA plot of the Yangtze River. (2) The PCA loading plot of water quality parameters. (3) The scree plot for explained variances using the principal components. Red represents spring, blue is summer, yellow is autumn, and green is winter.

**4. Discussion**

*4.1. Causes Affecting the Spatiotemporal Distributions of Individual Water Quality Parameters*

The water quality of Yangtze River’s main stream displayed clear spatiotemporal trends based on physicochemical characteristics. Between July and October, concentrations of COD<sub>Mn</sub>, T, TUR, and TP were higher than in other months, but DO showed a trend in the reverse direction. The pH, EC, and TUR decreased from upstream to downstream, while TN showed the opposite spatial variation.

Water temperature is the main factor affecting the change in dissolved oxygen [56]. The higher the temperature, the lower the dissolved oxygen concentrations. Consumed by organisms in water [43], dissolved oxygen is closely related to the water quality. Due to the rainy season, which lasts from July to November, the organic stuff that chemical fertilizers and pesticides create is washed into the water body. On the other hand, the relatively high

temperature will also cause inhabitants' water use to rise, increasing the pollution load from home sources [57]. Pesticides, fertilizers, and domestic sewage contain a lot of organic pollutants, so  $\text{COD}_{\text{Mn}}$  and TP concentrations were greater from July to October. This is consistent with other studies [28,58]. During the rainy season, non-point source pollution will contribute to water quality at a higher rate [57]. Therefore, the government can reduce the impact of non-point source pollution on the Yangtze River's water quality by adjusting the structure of agricultural input, lowering the usage of fertilizers and pesticides, and expanding the local sewage treatment capacity.

One of the chemical factors that affects or causes the mineralization process brought on by the watershed's lithological composition is pH [48]. There was no significant change in pH, which may be influenced by carbonate rocks [59]. According to the China Ecological and Environmental Bulletin 2021, acid rain is mainly distributed in the south of the Yangtze River and in the eastern Yunnan–Guizhou Plateau. The Yangtze River is dominated by limestone and carbonate-rich Triassic sand shales [60], and acid rain speeds up the dissolving of these salt-bearing minerals, which was the cause of the pH being higher upstream. The EC value of the Yangtze River's main stream fell from the upper reaches to the lower reaches, and the upper reaches' high conductivity may be related to some sedimentary rocks' natural weathering. In surface water, TUR is usually caused by suspended sediments or algae. Suspended particles have a significant impact on the reduction in water clarity [61]. High TUR will lead to deterioration of water quality and increase the cost of nearby drinking water treatment with the Yangtze River water as raw water [9,62]. The Yangtze River's upper reaches have a wide longitudinal slope and vigorous flushing, which raises the channel's silt concentration and causes the TUR to be higher. It is worth noting the TUR value of the upstream LD monitoring station. The Yangtze River's yearly average TUR was 48.22 NTU, while the LD station's annual average TUR was 130.67 NTU, or nearly 2.7 times more. According to the data from China's second national pollution source census, the Yangtze River water body receives more than 50% of its nitrogen and phosphorus input from agricultural non-point sources. Additionally, the net anthropogenic nitrogen input in the downstream area is about three times that in the upstream area [63], which could result in frequent algal blooms.

#### 4.2. Assesses the Overall Water Quality Condition and Patterns

The 33 monitoring stations were grouped using a systematic cluster analysis. From the analysis's findings, the first and second sets of monitoring stations were situated in the middle and upper reaches of the Yangtze River, while the third group was situated downstream. The results were consistent with the geographical location, indicating that the Yangtze River's water quality presented gradual characteristics in different regions. There were variations in the Yangtze River's monitoring priority when combined with the PCA method. The results showed that the Yangtze River's water quality in summer was worse than that in other seasons, which may be affected by domestic sewage and natural pollution [55]. Spatially, the Yangtze River's water quality had progressively declined from upstream to downstream.

The Yangtze River's upper reaches have greater water quality than its lower reaches, which may be attributable to the effectiveness of soil and water conservation in the Yangtze River's middle and upper reaches. The Yangtze River basin's soil and water loss was 337,000 square kilometers in 2020, as predicted by the Announcement on Soil and Water Conservation in the Yangtze River basin (2020), down from 531,000 square kilometers in the late 1990s [64]. Upstream, the water quality increased further. As a comprehensive parameter of the degree of surface water organic matter pollution,  $\text{COD}_{\text{Mn}}$  could reflect both the organic matter content and the level of water quality pollution. The PCA method identified a correlation between  $\text{COD}_{\text{Mn}}$  and the middle–upper range, indicating a close relationship between water quality and organic pollution. Authorities still need to keep an eye on the water quality in the upper portions of the Yangtze River, despite the fact that it was better than it was in the lower reaches. The Yangtze River's upper reaches have

experienced a constant decline in river flow as a result of climate change and rising human water consumption [65]. This could cause the water quality to worsen, the surrounding ecological environment to be destroyed, and the ecological environment of the downstream water to be harmed.

The lower parts of the Yangtze River are vulnerable to flood disasters during the rainy season as a result of severe rainfall events [66], which have varied degrees of damage to water supply facilities and sewage discharge conditions. Due to the abundance of river discharge and sediments, the relationship was manifested between water quality and TUR. The lower parts of the Yangtze River have seen a reduction in total phosphorus emissions since 2017. However, our research found that water quality was still strongly correlated with total phosphorus [67], which may be related to the issue of phosphorus residues [68]. Economic variables may be linked to water quality [69]. Some studies showed that water quality improves with economic development and the availability of comprehensive water treatment facilities [70]. The findings of our study, however, showed that while the water quality is worse in the lower parts of the Yangtze River, the economic situation is better. We hypothesize that the worsening of water quality is a result of an increase in home sewage and industrial wastewater caused by the rapid economic expansion in the lower reaches of the Yangtze River [64]. Relevant results showed that industrial wastewater discharge has decreased since China's adoption of the River Chief System [71]. Notwithstanding, the water quality in the downstream regions was still worse than that in the upstream regions, reflecting the need for continued measures to improve the downstream water quality.

## 5. Conclusions

In this study, the results lead to the following conclusions:

(1)  $\text{COD}_{\text{Mn}}$ , T, TUR, and TP levels are comparatively high from July to September, and EC and TUR all showed a clear downward spatial trend. By changing the pattern of agricultural inputs and using fewer pesticides and fertilizers, government agencies can lessen the effect of non-point source pollution on the Yangtze River's water quality;

(2) The Yangtze River's water quality declined from upstream to downstream. A total of 85% of the monitoring stations have "good" levels of water quality, with WQI values ranging from 71.16 to 81.25. The government can continue to take soil and water conservation measures in the upper and middle reaches of the Yangtze River to maintain water quality. At the same time, the variations of river flow should be tracked and timely adjusted to keep the water's ability to self-purify;

(3) The Yangtze River's middle and upper reaches of water quality were found to be strongly correlated with  $\text{COD}_{\text{Mn}}$ , whereas the downstream reaches of water quality were strongly correlated with TUR, TP, T, and DO, according to the results of the PCA. The target objectives for improving the water quality in various monitoring areas are made simpler using PCA, which makes it easier to create various treatment programs for various Yangtze River locations.

**Author Contributions:** Conceptualization, Y.L.; Methodology, J.H.; Software, G.J.; Validation, G.J.; Formal analysis, J.H. and Y.L.; Investigation, J.X.; Resources, Y.Z.; Data curation, Y.Z.; Writing—original draft, J.L., J.G. and J.X.; Writing—review & editing, J.L.; Visualization, J.G.; Supervision, J.L.; Project administration, J.L.; Funding acquisition, J.L. All authors have read and agreed to the published version of the manuscript.

**Funding:** This project is funded by the Ministry of Education's "Chunhui Program" Collaborative Research Project of China (No. 202202135), the Key Technology R&D Program of Henan Province of China (No. 212102310953), the Scientific Development Program of Nanyang of China (KJGG016 and RKX006), and the Scientific Research Program of Nanyang Normal University (2023QN018).

**Data Availability Statement:** The data that support the findings of this study are available from the corresponding author upon reasonable request.

**Conflicts of Interest:** The authors declare no conflict of interest.

## References

1. Vörösmarty, C.J.; McIntyre, P.B.; Gessner, M.O.; Dudgeon, D.; Prusevich, A.; Green, P.; Glidden, S.; Bunn, S.E.; Sullivan, C.A.; Liermann, C.R.; et al. Global threats to human water security and river biodiversity. *Nature* **2010**, *467*, 555–561. [[CrossRef](#)]
2. Dudgeon, D.; Arthington, A.H.; Gessner, M.O.; Kawabata, Z.; Knowler, D.J.; Leveque, C.; Naiman, R.J.; Prieur-Richard, A.H.; Soto, D.; Stiassny, M.L.; et al. Freshwater biodiversity: Importance, threats, status and conservation challenges. *Biol. Rev. Camb. Philos. Soc.* **2006**, *81*, 163–182. [[CrossRef](#)] [[PubMed](#)]
3. Chang, D.; Lai, Z.; Li, S.; Li, D.; Zhou, J. Critical source areas' identification for non-point source pollution related to nitrogen and phosphorus in an agricultural watershed based on SWAT model. *Environ. Sci. Pollut. Res. Int.* **2021**, *28*, 47162–47181. [[CrossRef](#)] [[PubMed](#)]
4. Hayward, E.E.; Gillis, P.L.; Bennett, C.J.; Prosser, R.S.; Salerno, J.; Liang, T.; Robertson, S.; Metcalfe, C.D. Freshwater mussels in an impacted watershed: Influences of pollution from point and non-point sources. *Chemosphere* **2022**, *307*, 135966. [[CrossRef](#)] [[PubMed](#)]
5. Lu, J.; Zhang, Y.; Chen, M.; Wang, L.; Zhao, S.; Pu, X.; Chen, X. Estimation of monthly 1 km resolution PM<sub>2.5</sub> concentrations using a random forest model over “2 + 26” cities, China. *Urban Clim.* **2021**, *35*, 100734. [[CrossRef](#)]
6. Rodell, M.; Famiglietti, J.S.; Wiese, D.N.; Reager, J.T.; Beaulieu, H.K.; Landerer, F.W.; Lo, M.H. Emerging trends in global freshwater availability. *Nature* **2018**, *557*, 651–659. [[CrossRef](#)]
7. Zou, Z.; Xiao, X.; Dong, J.; Qin, Y.; Doughty, R.B.; Menarguez, M.A.; Zhang, G.; Wang, J. Divergent trends of open-surface water body area in the contiguous United States from 1984 to 2016. *Proc. Natl. Acad. Sci. USA* **2018**, *115*, 3810–3815. [[CrossRef](#)]
8. Pekel, J.F.; Cottam, A.; Gorelick, N.; Belward, A.S. High-resolution mapping of global surface water and its long-term changes. *Nature* **2016**, *540*, 418–422. [[CrossRef](#)]
9. Loi, J.X.; Chua, A.S.M.; Rabuni, M.F.; Tan, C.K.; Lai, S.H.; Takemura, Y.; Syutsubo, K. Water quality assessment and pollution threat to safe water supply for three river basins in Malaysia. *Sci. Total Environ.* **2022**, *832*, 155067. [[CrossRef](#)]
10. Bashir, I.; Lone, F.A.; Bhat, R.A.; Mir, S.A.; Dar, Z.A.; Dar, S.A. Concerns and Threats of Contamination on Aquatic Ecosystems. In *Bioremediation and Biotechnology: Sustainable Approaches to Pollution Degradation*; Hakeem, K.R., Bhat, R.A., Qadri, H., Eds.; Springer International Publishing: Cham, Switzerland, 2020; pp. 1–26. [[CrossRef](#)]
11. Kumar, P.; Gacem, A.; Ahmad, M.T.; Yadav, V.K.; Singh, S.; Yadav, K.K.; Alam, M.M.; Dawane, V.; Piplode, S.; Maurya, P.; et al. Environmental and human health implications of metal(loid)s: Source identification, contamination, toxicity, and sustainable clean-up technologies. *Front. Environ. Sci.* **2022**, *10*, 1–23. [[CrossRef](#)]
12. Zamparas, M.; Zacharias, I. Restoration of eutrophic freshwater by managing internal nutrient loads. A review. *Sci. Total Environ.* **2014**, *496*, 551–562. [[CrossRef](#)] [[PubMed](#)]
13. Wang, B.; Wang, Y.; Wang, S. Improved water pollution index for determining spatiotemporal water quality dynamics: Case study in the Erdao Songhua River Basin, China. *Ecol. Indic.* **2021**, *129*, 107931. [[CrossRef](#)]
14. Zhang, J.; Li, S.; Dong, R.; Jiang, C.; Ni, M. Influences of land use metrics at multi-spatial scales on seasonal water quality: A case study of river systems in the Three Gorges Reservoir Area, China. *J. Clean. Prod.* **2019**, *206*, 76–85. [[CrossRef](#)]
15. Jhariya, D.C.; Kumar, T.; Pandey, H.K.; Kumar, S.; Kumar, D.; Gautam, A.K.; Baghel, V.S.; Kishore, N. Assessment of groundwater vulnerability to pollution by modified DRASTIC model and analytic hierarchy process. *Environ. Earth Sci.* **2019**, *78*, 610. [[CrossRef](#)]
16. Su, K.; Wang, Q.; Li, L.; Cao, R.; Xi, Y.; Li, G. Water quality assessment based on Nemerow pollution index method: A case study of Heilongtan reservoir in central Sichuan province, China. *PLoS ONE* **2022**, *17*, e0273305. [[CrossRef](#)] [[PubMed](#)]
17. Zhong, C.; Yang, Q.; Liang, J.; Ma, H. Fuzzy comprehensive evaluation with AHP and entropy methods and health risk assessment of groundwater in Yinchuan Basin, northwest China. *Environ. Res.* **2022**, *204*, 111956. [[CrossRef](#)]
18. Kuo, Y.M.; Liu, C.W.; Lin, K.H. Evaluation of the ability of an artificial neural network model to assess the variation of groundwater quality in an area of blackfoot disease in Taiwan. *Water Res.* **2004**, *38*, 148–158. [[CrossRef](#)]
19. Feng, L.; Zhu, X.; Sun, X. Assessing coastal reclamation suitability based on a fuzzy-AHP comprehensive evaluation framework: A case study of Lianyungang, China. *Mar. Pollut. Bull.* **2014**, *89*, 102–111. [[CrossRef](#)]
20. Singh, Y.; Singh, G.; Khattar, J.S.; Barinova, S.; Kaur, J.; Kumar, S.; Singh, D.P. Assessment of water quality condition and spatiotemporal patterns in selected wetlands of Punjab, India. *Environ. Sci. Pollut. Res. Int.* **2022**, *29*, 2493–2509. [[CrossRef](#)]
21. Wallace, J.; Champagne, P.; Hall, G. Multivariate statistical analysis of water chemistry conditions in three wastewater stabilization ponds with algae blooms and pH fluctuations. *Water Res.* **2016**, *96*, 155–165. [[CrossRef](#)]
22. Xue, Y.; Ma, Y.; Long, G.; He, H.; Li, Z.; Yan, Z.; Wan, J.; Zhang, S.; Zhu, B. Evaluation of water quality pollution and analysis of vertical distribution characteristics of typical Rivers in the Pearl River Delta, South China. *J. Sea Res.* **2023**, *193*, 102380. [[CrossRef](#)]
23. Naskar, M.; Das Sarkar, S.; Raman, R.K.; Gogoi, P.; Sahu, S.K.; Chandra, G.; Bhor, M. Quantifying plankto-environmental interactions in a tropical river Narmada, India: An alternative model-based approach. *Ecohydrol. Hydrobiol.* **2020**, *20*, 265–275. [[CrossRef](#)]
24. Zhang, Y.; Sun, M.; Yang, R.; Li, X.; Zhang, L.; Li, M. Decoupling water environment pressures from economic growth in the Yangtze River Economic Belt, China. *Ecol. Indic.* **2021**, *122*, 107314. [[CrossRef](#)]
25. Xu, Y.; Wu, Y.; Zhang, X.; Yin, G.; Fu, Y.; Wang, X.; Hu, Q.; Hao, F. Contributions of climate change to eco-compensation identification in the Yangtze River economic Belt, China. *Ecol. Indic.* **2021**, *133*, 108425. [[CrossRef](#)]
26. Qiu, Q.; Dai, L.; Van Rijswick, H.F.M.W.; Tu, G. Improving the Water Quality Monitoring System in the Yangtze River Basin—Legal Suggestions to the Implementation of the Yangtze River Protection Law. *Laws* **2021**, *10*, 25. [[CrossRef](#)]



27. Chen, D.; Hou, L.-J.; Liao, Y.-D. Strengthening efficient usage, protection, and restoration of Yangtze River shoreline. *Water Sci. Eng.* **2021**, *14*, 257–259. [[CrossRef](#)]
28. Liu, S.; Fu, R.; Liu, Y.; Suo, C. Spatiotemporal variations of water quality and their driving forces in the Yangtze River Basin, China, from 2008 to 2020 based on multi-statistical analyses. *Environ. Sci. Pollut. Res. Int.* **2022**, *29*, 69388–69401. [[CrossRef](#)]
29. Wu, Y.; Fang, H.; Huang, L.; Cui, Z. Particulate organic carbon dynamics with sediment transport in the upper Yangtze River. *Water Res.* **2020**, *184*, 116193. [[CrossRef](#)]
30. Liu, Y.; Li, L. Multiple Evaluations of the Spatial and Temporal Characteristics of Surface Water Quality in the Typical Area of the Yangtze River Delta of China Using the Water Quality Index and Multivariate Statistical Analysis: A Case Study in Shengzhou City. *Int. J. Environ. Res. Public Health* **2023**, *20*, 2883. [[CrossRef](#)]
31. Di, Z.; Chang, M.; Guo, P. Water Quality Evaluation of the Yangtze River in China Using Machine Learning Techniques and Data Monitoring on Different Time Scales. *Water* **2019**, *11*, 339. [[CrossRef](#)]
32. Li, X.; Zhao, Q.; Li, A.; Jia, S.; Wang, Z.; Zhang, Y.; Wang, W.; Zhou, Q.; Pan, Y.; Shi, P. Spatiotemporal distribution and fates of neonicotinoid insecticides during the urban water cycle in the lower reaches of the Yangtze River, China. *Water Res.* **2022**, *226*, 119232. [[CrossRef](#)] [[PubMed](#)]
33. Yao, R.; Wang, L.; Gui, X.; Zheng, Y.; Zhang, H.; Huang, X. Urbanization Effects on Vegetation and Surface Urban Heat Islands in China's Yangtze River Basin. *Remote Sens.* **2017**, *9*, 540. [[CrossRef](#)]
34. Yang, X.; Meng, F.; Fu, P.; Zhang, Y.; Liu, Y. Spatiotemporal change and driving factors of the Eco-Environment quality in the Yangtze River Basin from 2001 to 2019. *Ecol. Indic.* **2021**, *131*, 108214. [[CrossRef](#)]
35. Yang, P.; Xia, J.; Luo, X.; Meng, L.; Zhang, S.; Cai, W.; Wang, W. Impacts of climate change-related flood events in the Yangtze River Basin based on multi-source data. *Atmos. Res.* **2021**, *263*, 105819. [[CrossRef](#)]
36. Li, Y.; Yan, D.; Peng, H.; Xiao, S. Evaluation of precipitation in CMIP6 over the Yangtze River Basin. *Atmos. Res.* **2021**, *253*, 105406. [[CrossRef](#)]
37. Qu, S.; Wang, L.; Lin, A.; Yu, D.; Yuan, M.; Li, C.a. Distinguishing the impacts of climate change and anthropogenic factors on vegetation dynamics in the Yangtze River Basin, China. *Ecol. Indic.* **2020**, *108*, 105724. [[CrossRef](#)]
38. Ministry of Environmental Protection of China. *Water Quality Sampling-Technical Regulation of the Preservation and Handling of Samples, China*; China Environmental Science Press: Beijing, China, 2009.
39. Ministry of Environmental Protection of China. *Standard Methods for the Examination of Water and Wastewater (Version 4)*; China Environmental Science Press: Beijing, China, 2002.
40. Pesce, S.F.; Wunderlin, D.A. Use of water quality indices to verify the impact of Córdoba City (Argentina) on Suquia River. *Water Res.* **2000**, *34*, 2915–2926. [[CrossRef](#)]
41. Kannel, P.R.; Lee, S.; Lee, Y.S.; Kanel, S.R.; Khan, S.P. Application of water quality indices and dissolved oxygen as indicators for river water classification and urban impact assessment. *Environ. Monit. Assess.* **2007**, *132*, 93–110. [[CrossRef](#)]
42. Zhao, P.; Tang, X.; Tang, J.; Wang, C. Assessing Water Quality of Three Gorges Reservoir, China, Over a Five-Year Period From 2006 to 2011. *Water Resour. Manag.* **2013**, *27*, 4545–4558. [[CrossRef](#)]
43. Nong, X.; Shao, D.; Zhong, H.; Liang, J. Evaluation of water quality in the South-to-North Water Diversion Project of China using the water quality index (WQI) method. *Water Res.* **2020**, *178*, 115781. [[CrossRef](#)]
44. Cude, C.G. Oregon water quality index a tool for evaluating water quality management Effectiveness<sup>1</sup>. *JAWRA J. Am. Water Resour. Assoc.* **2001**, *37*, 125–137. [[CrossRef](#)]
45. Li, M.; Liu, Z.; Zhang, M.; Chen, Y. A workflow for spatio-seasonal hydro-chemical analysis using multivariate statistical techniques. *Water Res.* **2021**, *188*, 116550. [[CrossRef](#)] [[PubMed](#)]
46. Mora, A.; Torres-Martinez, J.A.; Moreau, C.; Bertrand, G.; Mahlknecht, J. Mapping salinization and trace element abundance (including As and other metalloids) in the groundwater of north-central Mexico using a double-clustering approach. *Water Res.* **2021**, *205*, 117709. [[CrossRef](#)] [[PubMed](#)]
47. Mandel, P.; Maurel, M.; Chenu, D. Better understanding of water quality evolution in water distribution networks using data clustering. *Water Res.* **2015**, *87*, 69–78. [[CrossRef](#)]
48. Bengraine, K.; Marhaba, T.F. Using principal component analysis to monitor spatial and temporal changes in water quality. *J. Hazard. Mater.* **2003**, *100*, 179–195. [[CrossRef](#)]
49. Olsen, R.L.; Chappell, R.W.; Loftis, J.C. Water quality sample collection, data treatment and results presentation for principal components analysis—literature review and Illinois River Watershed case study. *Water Res.* **2012**, *46*, 3110–3122. [[CrossRef](#)]
50. Kurunc, A.; Yurekli, K.; Okman, C. Effects of Kilickaya Dam on concentration and load values of water quality constituents in Kelkit Stream in Turkey. *J. Hydrol.* **2006**, *317*, 17–30. [[CrossRef](#)]
51. Ministry of Environmental Protection of China. *Environmental Quality Standards for Surface Water*; Ministry of Environmental Protection of China: Beijing, China, 2002.
52. Yang, J.; Yu, X.; Liu, L.; Zhang, W.; Guo, P. Algae community and trophic state of subtropical reservoirs in southeast Fujian, China. *Environ. Sci. Pollut. Res. Int.* **2012**, *19*, 1432–1442. [[CrossRef](#)]
53. Pu, W.; Quan, W.; Ma, Z.; Shi, X.; Zhao, X.; Zhang, L.; Wang, Z.; Wang, W. Long-term trend of chemical composition of atmospheric precipitation at a regional background station in Northern China. *Sci. Total Environ.* **2017**, *580*, 1340–1350. [[CrossRef](#)]
54. Warsito, B.; Sumiyati, S.; Yasin, H.; Faridah, H. Evaluation of river water quality by using hierarchical clustering analysis. *IOP Conf. Ser. Earth Environ. Sci.* **2021**, *896*, 012072. [[CrossRef](#)]

55. Wei, H.; Yu, H.; Zhang, G.; Pan, H.; Lv, C.; Meng, F. Revealing the correlations between heavy metals and water quality, with insight into the potential factors and variations through canonical correlation analysis in an upstream tributary. *Ecol. Indic.* **2018**, *90*, 485–493. [[CrossRef](#)]
56. Benson, B.B.; Krause, D., Jr. The concentration and isotopic fractionation of oxygen dissolved in freshwater and seawater in equilibrium with the atmosphere<sup>1</sup>. *Limnol. Oceanogr.* **1984**, *29*, 620–632. [[CrossRef](#)]
57. Bai, H.; Chen, Y.; Wang, Y.; Song, Z.; Tong, H.; Wei, Y.; Yu, Q.; Xu, Z.; Yang, S. Contribution rates analysis for sources apportionment to special river sections in Yangtze River Basin. *J. Hydrol.* **2021**, *600*, 126519. [[CrossRef](#)]
58. Qu, X.; Chen, Y.; Liu, H.; Xia, W.; Lu, Y.; Gang, D.D.; Lin, L.S. A holistic assessment of water quality condition and spatiotemporal patterns in impounded lakes along the eastern route of China's South-to-North water diversion project. *Water Res.* **2020**, *185*, 116275. [[CrossRef](#)] [[PubMed](#)]
59. Sener, S.; Sener, E.; Davraz, A. Evaluation of water quality using water quality index (WQI) method and GIS in Aksu River (SW-Turkey). *Sci. Total Environ.* **2017**, *584–585*, 131–144. [[CrossRef](#)]
60. Jingsheng, C.; Feiyue, W.; Xinghui, X. Geochemistry of water quality of the Yangtze River basin. *Earth Sci. Front.* **2006**, *1*, 74–85.
61. Yan, R.; Li, L.; Gao, J. Framework for quantifying rural NPS pollution of a humid lowland catchment in Taihu Basin, Eastern China. *Sci. Total Environ.* **2019**, *688*, 983–993. [[CrossRef](#)]
62. Lee, C.S.; Lee, Y.C.; Chiang, H.M. Abrupt state change of river water quality (turbidity): Effect of extreme rainfalls and typhoons. *Sci. Total Environ.* **2016**, *557–558*, 91–101. [[CrossRef](#)]
63. Yao, M.; Hu, M.; Chen, D. Dynamic of net anthropogenic nitrogen inputs and riverine nitrogen export in the Yangtze River Basin in 1980–2015. *Environ. Sci.* **2021**, *42*, 5777–5785. [[CrossRef](#)]
64. Duan, W.; He, B.; Chen, Y.; Zou, S.; Wang, Y.; Nover, D.; Chen, W.; Yang, G. Identification of long-term trends and seasonality in high-frequency water quality data from the Yangtze River basin, China. *PLoS ONE* **2018**, *13*, e0188889. [[CrossRef](#)]
65. Shi, R.; Wang, T.; Yang, D.; Yang, Y. Streamflow decline threatens water security in the upper Yangtze river. *J. Hydrol.* **2022**, *606*, 127448. [[CrossRef](#)]
66. Yu, Z.; An, Q.; Liu, W.; Wang, Y. Analysis and evaluation of surface water changes in the lower reaches of the Yangtze River using Sentinel-1 imagery. *J. Hydrol. Reg. Stud.* **2022**, *41*, 101074. [[CrossRef](#)]
67. Qi, W.; Wang, X.; Kang, J.; Bai, Y.; Bian, R.; Xue, H.; Chen, L.; Guan, A.; Pan, Y.-R.; Liu, H.; et al. Improvement of the Yangtze River's Water Quality with Substantial Implementation of Wastewater Services Infrastructure Since 2013. *Engineering* **2023**, *21*, 135–142. [[CrossRef](#)]
68. Chen, D.; Shen, H.; Hu, M.; Wang, J.; Zhang, Y.; Dahlgren, R.A. Legacy Nutrient Dynamics at the Watershed Scale: Principles, Modeling, and Implications. *Adv. Agron.* **2018**, *149*, 237–313. [[CrossRef](#)]
69. Zhao, Z.; Zhang, L.; Deng, C. Changes in net anthropogenic nitrogen and phosphorus inputs in the Yangtze River Economic Belt, China (1999–2018). *Ecol. Indic.* **2022**, *145*, 109674. [[CrossRef](#)]
70. Wang, J.; Da, L.; Song, K.; Li, B.L. Temporal variations of surface water quality in urban, suburban and rural areas during rapid urbanization in Shanghai, China. *Environ. Pollut.* **2008**, *152*, 387–393. [[CrossRef](#)]
71. She, Y.; Liu, Y.; Jiang, L.; Yuan, H. Is China's River Chief Policy effective? Evidence from a quasi-natural experiment in the Yangtze River Economic Belt, China. *J. Clean. Prod.* **2019**, *220*, 919–930. [[CrossRef](#)]

**Disclaimer/Publisher's Note:** The statements, opinions and data contained in all publications are solely those of the individual author(s) and contributor(s) and not of MDPI and/or the editor(s). MDPI and/or the editor(s) disclaim responsibility for any injury to people or property resulting from any ideas, methods, instructions or products referred to in the content.